

RESEARCH ARTICLE

High-temperature response of geopolymer concrete: Influence of silica fume content and fiber type on mechanical and structural integrity

Haluk Görkem Alcan*

Kafkas University, Department of Civil Engineering, Kars, Türkiye

Article History

Received 19 April 2025 Accepted 24 June 2025

Keywords

Geopolymer concrete Basalt fiber Polymer fiber High temperature

Abstract

Geopolymer concrete has recently attracted increasing attention as an alternative to traditional concrete due to its low carbon emissions and environmental friendliness. In addition, geopolymer concrete has great potential due to the use of industrial waste materials in its mixture and its high performance. The aim of this study is to experimentally investigate the effects of adding 0%, 10% and 20% silica fume instead of granulated blast furnace slag in the geopolymer mixture and 1% basalt fiber and polymer fiber addition on the performance of geopolymer concrete under high temperatures. In the study, both dry unit weight and water absorption rate for the evaluation of physical properties and compressive and flexural strength properties for the evaluation of mechanical performance were investigated in detail. 212 cube and 108 prism samples with dimensions of 50x50x50 mm and 40x40x160 mm were produced, respectively. Samples were exposed to temperatures of 20°C, 100°C, 200°C, and 400°C, and compressive strength, flexural strength, mass loss, and load-deflection curves were analyzed. The results obtained showed that although the temperature increased up to 100°C, causing the strength to increase by 25%, the strength of the samples decreased by 70% at a temperature of 400°C. In addition, it was observed that the strength of the samples decreased with the increase of the SF ratio in the mixtures, but the use of polymer fibers balanced the mentioned negative effect. These findings show that durable and sustainable building materials can be produced under high temperature conditions when the SF and fiber type are optimized together. The study contributes to the material design for applications requiring high temperature resistance.

1. Introduction

Geopolymer is a new type of concrete made without cement and instead uses a binding system that uses alkali to harden it instead of traditional Portland cement. The system that binds this concrete together is formed by reacting industrial or agricultural wastes, or natural resources a high content of aluminum and silicon (fly ash, granulated blast furnace slag, metakaolin, volcanic tuff, marble dust), with alkali activators including sodium hydroxide (NaOH) and sodium silicate (Na₂SiO₃). The alkali-activated geopolymeric

^{*} Corresponding author (hgorkemalcan@kafkas.edu.tr)
eISSN 2630-5763 © 2025 Authors. Publishing services by golden light publishing®.

This is an open-access article under the CC BY-NC-ND license (http://creativecommons.org/licenses/by-nc-nd/4.0/).

structure is an amorphous or semi-crystalline aluminosilicate network system that gives rise to mechanical strength of concrete, acting like conventional cement hydrates by giving a binder system [1-5].

The most important advantage of geopolymer concrete is that it significantly reduces carbon emissions because it does not use Portland cement in its production. Since the cement industry is responsible for approximately 7% of global CO₂ emissions, geopolymer concrete has great potential for environmental sustainability [6-8]. In addition, this type of concrete can exhibit superior engineering properties such as high early and final compressive strength, good acid and sulphate resistance, and high temperature resistance. In addition, the durability and low permeability of geopolymer concrete make it suitable for use in infrastructure projects, industrial floor coverings, and structural elements exposed to high temperatures [9-11]. However, like any new material, there are also some challenges related to geopolymer concrete. For one, the mix design and optimization of alkali activator ratios can be complex, and thus, no standardized procedure has been widely accepted by industry yet. Moreover, fresh concrete properties like workability and setting time may range greatly based on raw material and mixing conditions. These challenges are being overcome thanks to research, and geopolymer concrete is taking its place among sustainable building materials [12-14].

Different types of fibers (steel, glass, carbon, polypropylene, basalt, etc.) when incorporated into conventional geopolymer concrete matrices yield construction material with enhanced mechanical and durability properties, commonly referred to as fibrous geopolymer concrete. Due to the random distribution of fibers in the geopolymer matrix and the restriction of crack propagation, this kind of concrete contributes not only high compressive strength but also high tensile, flexural, and impact resistance. Similar to conventional fiber concrete based on cement, the main task of the fibers added to the mixture is to control the formed microcracks and to provide a more ductile behavior by reducing the brittleness of the concrete. These attributes are particularly useful in constructions susceptible to earthquake effects, prefabricated components, precast elements, high temperature resistance applications, and infrastructure systems subjected to corrosive environmental conditions [15-20]. Not only does fiber geopolymer concrete have better mechanical properties, but it also has better environmental durability. With the fiber additive, this type of concrete can reduce the surface area of cracks, which helps prevent the penetration of harmful ions, while having a high resistance against chemical effects such as sulfate, chloride ions, or acid attacks. It is also a major plus when it comes to fire resistance. Thereby, explosive spalling on one hand can be prevented by the adhesion of micro channels formed as a result of the melting of the polypropylene fibers at certain temperature ranges by reducing the internal pressure at high temperatures. Because of this, fiber geopolymer concrete has emerged as an effective solution in applications such as tunnel linings, nuclear energy facilities, and fire-resistant wall panels [21,22].

The influence of fiber admixture on geopolymer concrete relies on the precise selection of fiber type, volume proportion, aspect ratio, and evenly dispersed distribution. For instance, steel fibers enhance flexural and impact strength considerably when reinforced to tensile strength, while glass and basalt fibers provide a lighter alternative with improved corrosion resistance. Since polypropylene has a specific gravity of less than one, it also aids in preventing plastic shrinkage cracks and helps with increasing fire resistance. It is proven in the literature that the ductility and energy absorption capacity of the geopolymer concrete increase significantly at even low fiber ratios (0.5–1.5%). They also modify the stress distribution at the tips of cracks, delay the consolidation and propagation of cracks, and finally avoid the sudden rupture of the concrete, making it present a more ductile behavior [23-25]. Besides, the impact of fiber additives on fresh concrete is another key issue. In general, the incorporation of fiber decreases the workability of the mixture, requiring more intensive mixing. In those cases, the fibers tend to tighten or are not obtained homogeneously distributed, thus in geopolymer compositions with low water/binder ratios [26-28]. Hence, the inclusion of superplasticizers and optimal mixing times becomes highly critical. The interaction of the alkaline environment with the fibers also needs to be carefully considered. Some glass fibers, e.g., e-glass, are known

to lose strength in the long term in highly alkaline environments, whereas basalt fibers tend to be more durable. Thus, in addition to the mechanical contributions, fiber selection should be tailored to provide optimal long-term performance [29-31].

The behavior of geopolymer concrete against high temperature effects is one of the most striking features of this type of concrete. While high temperatures in traditional Portland cement-based concretes, especially above 300°C, can cause significant strength losses, microstructure deterioration, and sudden and dangerous damages such as explosive spalling, geopolymer concrete exhibits a much more resistant performance against high temperatures due to its chemical structure. This resistance is mainly due to the amorphous or semi-crystalline aluminosilicate network structure of the geopolymer matrix. This structure is more thermally stable and can largely maintain its binder system even at high temperatures [32-35]. The performance of geopolymer concrete in the temperature range of 200-800°C can typically be addressed in three phases. Free water evaporation usually occurs in the first stage between 200-300°C. At this temperature level, a limited loss of strength or, in some cases, temporary increases in strength can be observed. This increase is linked to the evacuation of water from the microstructure, reducing porosity and densifying the matrix. However, above 400°C, loss of bound water and the formation of microstructure cracks and thermal expansion differences lead to a reduction of compressive strength. This loss of strength is particularly pronounced at 600°C and above, but it is usually still less pronounced than with cementitious-based concretes [36-42]. The strength of geopolymer concrete in a high temperature environment is influenced by various factors such as the type of aluminosilicate source, such as fly-ash or slag, the chemical composition of the binder, type and ratio of alkali activator, curing method, type of aggregate used in the mixture, and the types of fibers used if any. Mixtures including granulated blast furnace slag (GBFS) are more beneficial with respect to high temperature resistance since they comprise a denser and tightly structured material, comparable to fly ashbased materials. In addition, the potential effect of basalt or polypropylene fiber additives is positive for cracking, bursting peeling under high temperature [43-46].

Although prior studies have examined granulated blast furnace slag, silica fume, and fiber effects separately, their combined influence under high temperatures remains underexplored. This study fills that gap by evaluating how different fiber types and SF ratios jointly affect the mechanical and thermal behavior of geopolymer concrete, offering guidance for mix optimization in heat-exposed environments. This paper investigates the effects of high temperature (100, 200, and 400°C) and fiber type (basalt and polymer), and silica fume content on the mechanical and physical properties of geopolymer concrete through 212 cubes and 108 prism samples. Silica fume was used as a replacement for GBFS at 0%, 10% and 20% and the fiber volume was used at 1% for all samples. 24-hour compressive strength and flexural strength tests were performed to assess the effects of silica fume content and fiber type on the mechanical properties of the geopolymer concrete. Three-point flexural test was applied to determine the load-deflection curves and energy dissipation capacity of samples. Moreover, dry unit weight and water absorption capacity of the tested samples were obtained to determine the physical properties of geopolymer concrete. The compressive strength loss and mass loss results of the tested samples after exposure to high temperature were also investigated experimentally.

2. Experimental program

2.1. Materials

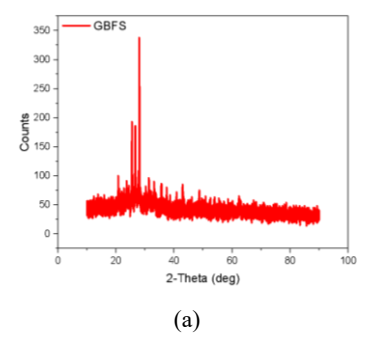
In this study, granulated blast furnace slag (GBFS) was used as the main binder material for the production of geopolymer concrete. Blast furnace slag is generally a by-product obtained during the production phase in iron and steel plants. GBFS used in the mixture complies with ASTM C618 [47] standard. The chemical and physical properties of GBFS are presented in Table 1. XRD pattern and particle size of GBFS are shown

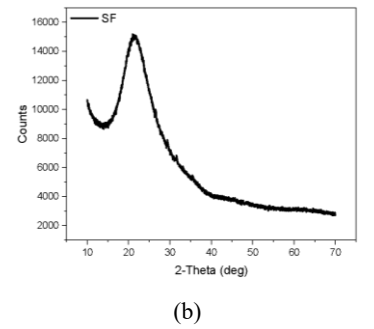
in Fig. 1a and Fig. 2a, respectively. The XRD pattern of the GBFS is characterized by its amorphous nature, as evidenced by a broad hump in the 20°–35° range. This indicates the dominance of the glassy phase and confirms that the slag predominantly possesses a vitreous-amorphous structure. The image of GBFS used in the geopolymer mix is shown in Fig. 3. The specific gravity and specific surface area of GBFS are 2.88 g/cm³ and 5445 cm²/g, respectively.

In the study, silica fume (SF) was used instead of GBFS at three different rates (0%, 10% and 20%) to investigate the effect on the physical, mechanical, and thermal properties of the mixtures. The chemical of SF is presented in Table 1. The specific gravity of silica fume is 2.25 g/cm³, and the fineness modulus is 21.2 m²/g. The XRD pattern and particle size analysis of SF are presented in Fig. 1b and Fig. 2a, respectively. XRD pattern of SF (silica fume) exhibits an amorphous character rather than a crystalline one, as the absence of distinct peaks confirms the glassy nature of the nanosized spherical SiO2 particles. The image of SF used in the geopolymer mix is shown in Fig. 3. Two different materials, sand and quartz, were used as fine aggregate in the geopolymer concrete mixture. The specific gravity of the quartz material is 2.71 g/cm³. In addition, the chemical properties of the quartz material are presented in Table 1. The XRD pattern and particle analysis of the quartz material are shown in Fig. 1c and Fig. 2b, respectively. The XRD pattern of quartz presents an entirely different structure from GBFS and SF; the presence of sharp and well-defined peaks reflects a highly crystalline structure. In particular, the intense peak around 25° indicates the high crystalline purity of the material. This crystalline structure suggests that quartz sand behaves as an inert filler and would participate only minimally in chemical reactions within binder systems. In addition, the specific gravity of the sand is 2.65 g/cm³. Particle size analysis of sand is shown in Fig. 2c. The images of quartz and sand as fine aggregate are shown in Fig. 3.

Table 1. Chemical and physical properties of GBFS, SF, and Quartz (%)

1 3 1 1	, ,	()	
Property	GBFS	SF	Quartz
SiO ₂	37.8	94.8	97.2
CaO	34.6	0.4	-
Al_2O_3	10.5	0.4	12.4
MgO	7.9	0.7	< 0.1
Fe_2O_3	3.4	0.9	0.3
SO_3	2.5	0.3	-
K_2O	0.8	0.6	-
Na_2O	0.6	0.4	-
LOI	0.4	-	-
Specific gravity (g/cm ³)	2.88	2.25	2.71
Setting time (Initial/Final)	155/230	-	-





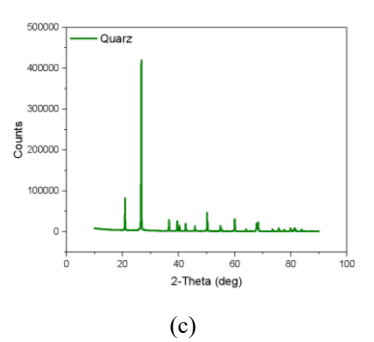


Fig. 1. XRD pattern of (a) GBFS, (b) SF, (c) quartz

Alcan Alcan

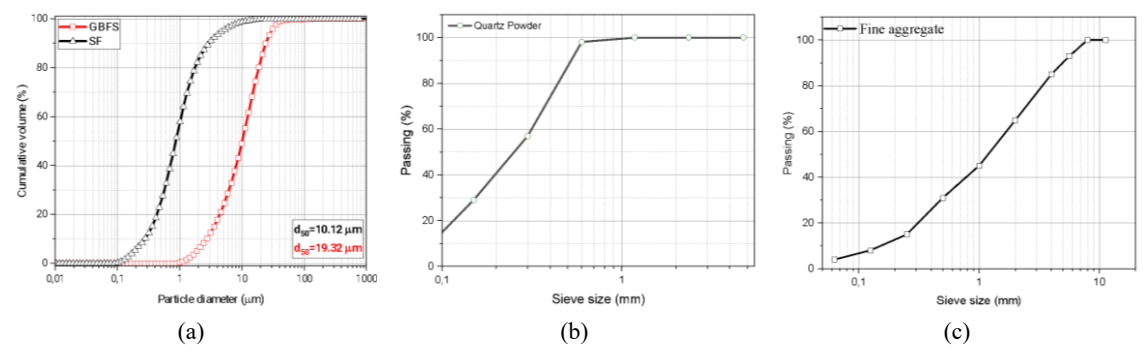


Fig. 2. Particle size analysis of (a) GBFS and SF, (b) quartz, (c) fine aggregate

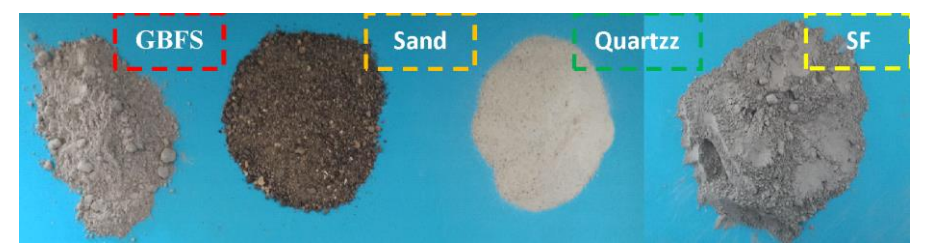


Fig. 3. Image of materials used in geopolymer mix

In the fibrous samples, two different fiber types, basalt (BF) and polymer (PF), were used at a constant rate of 1%. The technical specifications of BF and PF are presented in Table 2. It was aimed to benefit from the high strength and chemical resistance of BF and PF randomly distributed in the geopolymer matrix. The length of BF and PF is 12 mm. The specific gravity of BF and PF is 2.7 and 1 g/cm³, respectively.

Sodium silicate (Na₂SiO₃) and sodium hydroxide (NaOH) were used as alkali activators in the geopolymer composite. Sodium silicate and sodium hydroxide were used in the mixture to initiate the reactions of the geopolymer composite. The Na₂SiO₃/NaOH ratio was preferred as 2.5 based on past studies and the fluidity of the mixtures [48-50]. The density of NaOH at 30 °C is 1.2 g/cm³, and the boiling point is 1390 °C. The density of Na₂SiO₃ at 20 °C is 1.42 g/cm³. In addition, the purity level is 2 modules. The technical properties of NaOH and Na₂SiO₃ are shown in Table 3.

Table 2. Technical properties of BF and PF

Property	BF	PF
Tensile strength (MPa)	4840	800-1100
Melting temperature (°C)	1450	255~265
Diameter (μ m)	9-23	17-21
Length (mm)	12	12
Specific gravity (g/cm ³)	2.7	1
Elastic modulus (GPa)	89	-
Temperature limit (°C)	-250 ~ +950	-
Image		וע

Table 3. Chemical con	nponents of NaOH	and Na ₂ SiO ₃
-----------------------	------------------	--------------------------------------

	NaOH	Na ₂ CO ₃	Cl	SO ₄	Al	Fe	SiO ₂	Na ₂ O	H ₂ O
NaOH	98	0.2	< 0.01	< 0.01	< 0.01	< 0.01	-	-	-
Na ₂ SiO ₃	-	-	-	-	-	< 0.01	28.4	8.6	62.2

2.2. Mix and sample preparation

In this study, three different geopolymer concrete mixtures based on GBFS were produced. The number of components used in geopolymer mixes is depicted in Table 4. Mixing ratios were created based on past studies [51-53].

In the first geopolymer mixture (Mix-1). In the second (Mix-2) and third mixtures (Mix-3), SF was used by replacing GBFS. In Mix-2 and Mix-3, SF was replaced with GBFS by 10% and 20%, respectively. Sand and quartz materials were used as fine aggregates. In addition, NaOH and Na₂SiO₃ were used as alkali activators.

The concrete casting processes of the samples were carried out at the Civil Engineering Laboratory at Atatürk University. All samples were carried out in a laboratory environment and with a 5 dm³ capacity mixer. Concrete casting was carried out in three steps. In the first step, solid materials (GBFS, SF, and aggregates) were mixed at 145 rpm for 2 minutes. In the second step, basalt/polymer fibers were added to the mixture and mixed for another 2 minutes at 145 rpm. In the third step, alkali activators were added to the mixture and mixed for another 2 minutes at 280 rpm. After the mixture was prepared, it was poured into steel molds. After the geopolymer concrete mixtures were poured into the molds, they were wrapped in stretch. All samples were cured at 60°C for 4 hours after production. After the heat curing, the samples were kept in the laboratory until the test day. The images of the heat-cured and kept in the laboratory are presented in Fig. 4. The schematic of the process from the production process of the samples to the testing day is presented in Fig. 5.

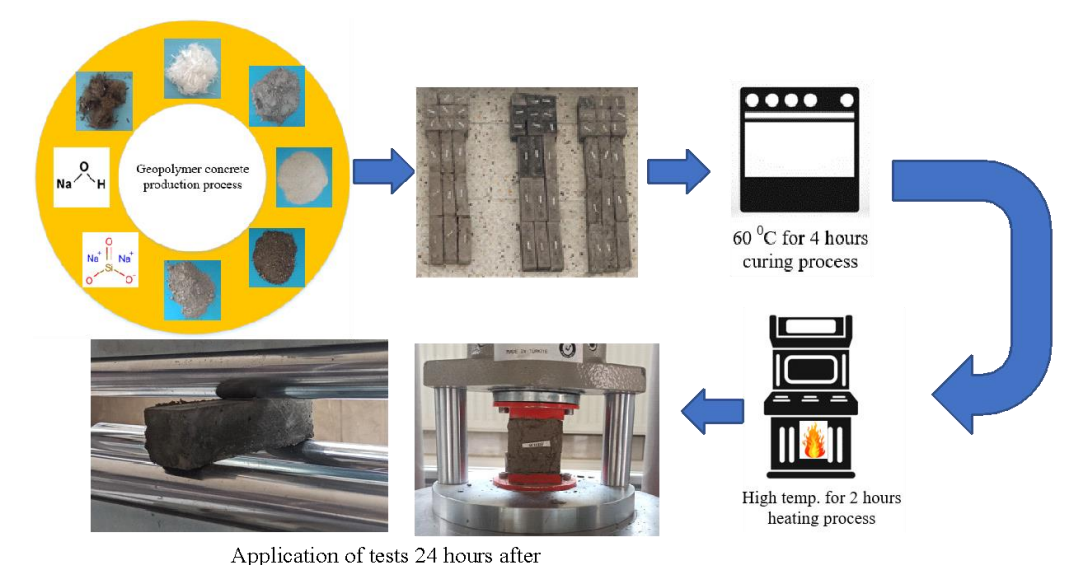
Table 4. Materials proportions of geopolymer mixes (kg/m³)

Material	Mix-1 (0%SF)	Mix-2 (10%SF)	Mix-3 (20%SF)
GBFS	700	630	560
SF	-	70	140
Sand	593	582	571
Quartz	404	394	390
NaOH	148	148	148
Na ₂ SiO ₃	370	370	370





Fig. 4. Images of tested samples after casting



production of samples

Fig. 5. The schematic of the process of the tested samples

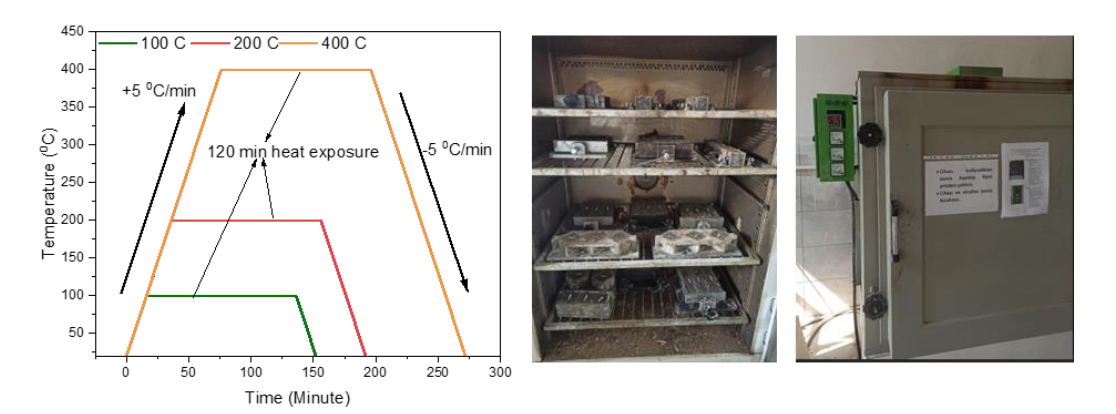


Fig. 6. High temperature process

One of the aims of this study is to determine the loss of compressive strength and mass loss after the high temperature effect on the samples. Therefore, high temperatures of 100°C, 200°C, and 400°C were applied to the samples. The temperature procedure applied to the samples and the picture of the samples are presented in Fig. 6. The temperature effect was applied to the samples in the laboratory environment with the help of an oven. The samples were exposed to a temperature increase of +5°C/min until the target temperature. After reaching the target temperature, all samples were exposed to high temperatures for 120 minutes. Then, all samples were cooled in the oven at 5°C/min.

Sample parameters were used when labelling the samples. The first letter of the labelling indicates the SF ratio of the sample. SF0, SF10, and SF20 represent 0%, 10% and 20% FS ratio, respectively. The fiber content of the sample is shown in the second row. NF, BF, and PF represent Non-Fiber, Basalt Fiber, and Polymer Fiber samples, respectively. The temperature value to which the samples were exposed is shown in the last row. For example, the SF20/BF/200 naming indicates that the SF ratio is 10% and the basalt fiber sample is exposed to 200°C.

2.3. Testing procedures

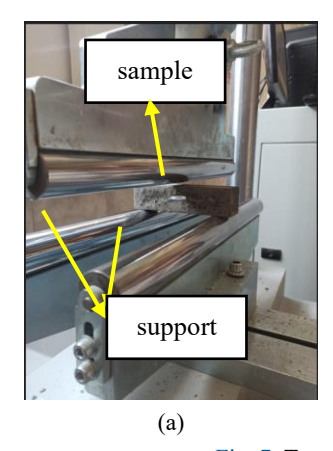
The three-point flexural test was applied to prism samples with dimensions of 40x40x160 mm according to the ASTM C348-19 [54] standard to evaluate the flexural strength of the tested samples. The flexural test setup is presented in Fig. 7a. The load-displacement curves of the flexural test applied samples were plotted. Cube samples with dimensions of 50×50×50 mm were used to investigate compressive strength. The compressive strength test setup applied according to ASTM C349-18 [55] standard is presented in Fig. 7b. Transport properties of geopolymer concrete were assessed on the specimens with a 50×50×50 mm size after 24 hours. The tests to determine the transport properties were performed according to the ASTM C642-13 [56], such as dry unit weight and water absorption capacity (as seen from Fig. 7c). Both the compressive strength loss and weight loss results of the tested samples after high temperature exposure were also calculated. Three of the samples were produced, and the average of the three samples was used in the relevant tables and graphs. In addition, all samples were subjected to the relevant test 24 hours after production.

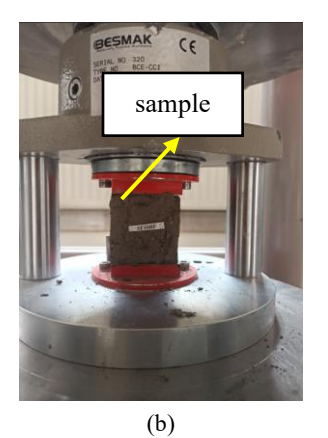
3. Results and discussion

This section evaluates the physical properties (water absorption and dry density), mechanical properties (compressive strength, flexural strength), and durability performance (high-temperature resistance) test results.

3.1. Physical properties

The dry unit weight and water absorption rate results of the samples are presented in Fig. 8. It is seen that both the SF ratio in the mixture and the fiber type have an effect on the dry unit weight. From Fig. 8a, the increase in the SF ratio in the mixture generally decreased the dry unit weight. For example, while the average unit weight of the mixtures containing 0% SF (SF0) was 2186.7 kg/m³, when the SF ratio was increased to 20%, this value decreased to an average of 2125.3 kg/m³. This supports the effect of SF addition in reducing the unit weight. First of all, since the specific gravity of SF (2.25 g/cm³) is lower than the specific gravity of GBFS (2.88 g/cm³), the increase in the SF ratio in the mixture decreased the dry unit weight. SF has very fine particles with a fineness modulus of 21.2 m²/g. SF has increased workability due to its fine particle size. However, SF can cause a porous structure in the matrix. The increased porous structure in the matrix caused a decrease in dry unit weight. The increase in the SF ratio in the mixture also caused an increase in porosity and, therefore, a decrease in dry unit weight.





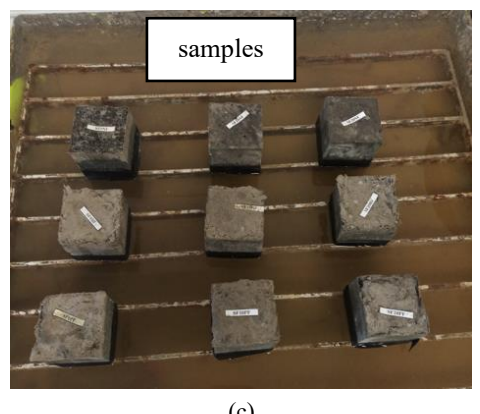


Fig. 7. Test setup for (a) flexural, (b) compressive, (c) absorption properties

SF is a very fine-grained (very high specific surface) pozzolanic material, which increases the activator requirement of the mixture and reduces workability. Under sufficient time, sufficient humidity, appropriate pH balance, and sufficient temperature parameters, SF has a high ability to chemically react. The 60°C temperature cure applied to the samples after the casting process for 4 hours may not have created suitable conditions for SF to fully react. This means that there may have been unreacted SF particles in the matrix. For geopolymerization to occur in the matrix, the pH value of the medium must be high (>12). Although high pH is sufficient for SF to dissolve, the geopolymerization reaction between dissolved silica and alumina must be completed for the reaction to continue. If the curing conditions are not suitable, SF particles may not contribute sufficiently to the formation of the binding gel. Unreacted SF particles and insufficient binding lead to the following results: (i) Low-adherence transition zones may form around SF particles. (ii) Microcracks and voids may form in these weak zones. (iii) Due to the high fineness of SF, porous structure formation may increase despite the increased water demand. (iv) Voids formed around unreacted SF grains after curing cause high porosity. Short-term heat curing and limited reaction of silica fume in a high alkaline environment cause SF to act as a "filler" instead of a binder. This increases void formation in transition zones and causes both a decrease in unit weight and an increase in water absorption rate. This effect can be optimized with long curing times or different activator ratios. Sevinc and Durgun [57] also stated that increasing the SF ratio in the geopolymer mixture reduces the dry unit weight. Kumar et al. [58] and Zhu et al. [59] similarly reported that the use of SF in the geopolymer matrix or the increase in the SF ratio in the matrix caused a more porous structure and thus decreased the dry unit weight.

A similar effect to the SF ratio in the mixture was observed in the fiber type. The fiber type in the geopolymer mixture also affects the dry unit weight. The dry unit weight of the fiber-free samples is generally higher than the fiber samples. The reason for this situation may be that the fibers randomly distributed in the matrix in the fiber samples cause a porous structure in the matrix. Especially in the SF20BF20 sample (2136 kg/m³), the porosity-increasing effect of the fiber is observed. The specific gravity of PF is quite low (1.0). This caused the samples containing PF to have lower unit volume weights. For example, the SF20PF20 sample shows the lowest value with 2064 kg/m³. The volumetric coverage of low-density polymer fibers in the matrix increases the volume of the concrete without increasing its mass, which in turn reduces the density. As a result, the increase in the SF ratio in the mixture reduces the total specific gravity and compactness of the mixture, thus causing the dry unit weight to decrease. Fiber additives showed different effects on dry unit weight depending on the type of fiber used. While fiber-free samples had higher density, this value decreased significantly in samples using low-specific-gravity polymer fibers. This is related to both the physical properties of the fibers and their effects on the void structure in the mixture.

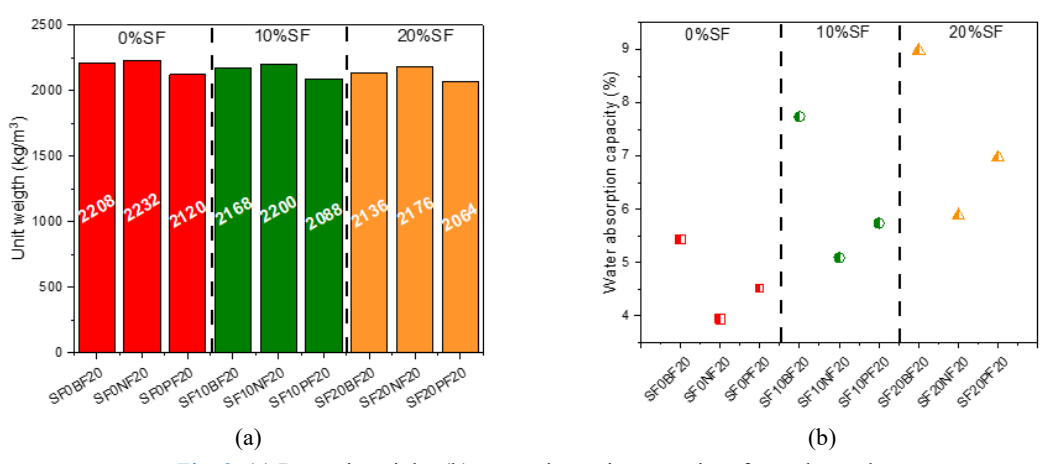


Fig. 8. (a) Dry unit weight, (b) water absorption capacity of tested samples

The water absorption capacity of the samples is directly related to the porosity and pore structure of the matrix. In addition, the water absorption capacity provides important information about the permeability and durability performance, and the microstructure of the samples. In this study, it is seen from Fig. 8b that both the SF ratio in the mixture and the fiber type are effective on the water absorption rate of the samples. The increase in the SF ratio increased the water absorption rate of the samples. This situation is related to the reasons mentioned above. In other words, since SF causes a porous structure in the matrix, it increases the water absorption capacity. Since the increase in the SF ratio limits the formation of the binder gel in the mixture, it causes the matrix to gain a more permeable structure. This permeability increases the water absorption capacity. Shariati et al. [60] and Rukzon et al. [61] stated that increasing the SF ratio in the mixture increases the water absorption capacity by approximately 29%.

The type of fiber used in the mixture affects the water absorption capacity since its distribution within the matrix is effective. The lowest water absorption rate was generally obtained in samples without fibers due to the more homogeneous and compact structure of the mixture. This situation has reduced the porosity of the samples and limited the water absorption capacity. Although basalt fibers have a high elastic modulus and high specific gravity, they can cause voids to form at the fiber-matrix interfaces when they are randomly distributed in the mixture. In addition, basalt fibers may cause microcracks after curing due to thermal expansion. The water absorption capacity of samples using polymer fibers is lower than those using basalt fibers. It is thought that the reason for this situation is that the flexibility of polymer fibers creates fewer microcracks compared to basalt fibers, and therefore, their water absorption rates are lower than BF. As a result, it was concluded that both the SF ratio and the fiber type have a significant effect on the water absorption capacity. The increase in the SF ratio caused water to penetrate more easily into the concrete due to the increase in the number of unreacted particles and micro porosity. Since basalt fibers cause microcracks at the matrix interface, water penetration is easier. The effect of polymer fibers on water absorption capacity was moderate. These findings show that the selection of SF ratio and fiber type should be made carefully to increase physical durability, and that especially high SF ratios and basalt fibers can cause negative effects in terms of permeability when used together. Haruna et al. [62] and Li et al. [63] reported that the increasing basalt fiber ratio in geopolymer concrete increased the water absorption capacity.

3.2. Mechanical properties

3.2.1. Compressive strength

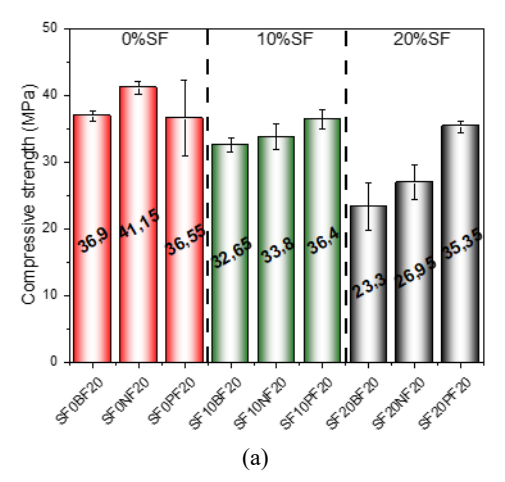
Compressive strength results are shown in Fig. 9. First of all, the effect of SF ratio on compressive strength was evaluated. Increasing the SF ratio from 0% to 10% in samples other than polymer fiber samples decreased the compressive strength. Increasing the SF ratio did not have a significant effect on compressive strength in polymer fiber samples. Increasing the SF content in fiber-free and basalt fiber samples caused the compressive strength to decrease by 17% and 11%, respectively. Increasing the SF ratio in the matrix limited the formation of binder gel at an early age (24 hours). As is known, a three-dimensional N-A-S-H network is formed at the end of the geopolymerization process in geopolymer concrete. The formation of this three-dimensional network occurs in three basic steps. In the first step, Si⁴⁺ and Al³⁺ ions are formed by dissolving SF and GBFS materials in a high pH environment. In the second step, these ions react with alkali activators during the polycondensation process and form the N-A-S-H network. In the third step, the N-A-S-H network hardens and forms the binder phase. In the 24 hours, the inclusion of SF in the above mechanism was slower. For this reason, the formation of the N-A-S-H network was slower. In this case, increasing the SF ratio from 0% to 10% caused a decrease in the compressive strength. Since GBFS contains both CaO and Al₂O₃, it causes the formation of N-A-S-H and C-A-S-H type binder gels. Since SF provides only silica in the matrix, the Al source in the matrix is limited. In other words, when the GBFS ratio in the mixture decreases and the

SF ratio increases, the compressive strength also decreases due to the decrease in the Al source. Moreover, SF could not react completely for 24 hours. In this case, it caused the formation of undissolved SF particles. Since the undissolved SF particles in the matrix cause a porous structure, they cause the formation of microcracks. The increase in the number of microcracks also caused the compressive strength to decrease. However, due to its high fineness and high reactivity, the curing time of SF is short, and it cannot fully participate in the geopolymer reaction under low temperature conditions to form binder gel, especially at early ages. It can put a huge drop in early age strength. A higher SF ratio shows more signatures of this effect. Thus, when applying SF, the curing time, ratios of activator and binder system balance shall be optimized with precaution.

Another reason why the increase in SF ratio decreases the compressive strength is thought to be the low adhesion between the insoluble SF particles in the matrix and the binder phase. Weak areas are formed due to the low adhesion between the insoluble SF particles and the binder phase. Microcracks form in these weak areas. Microcracks cause the integrity of the matrix to deteriorate, leading to a decrease in compressive strength. In samples containing polymer fibers, increasing the SF ratio from 0% to 10% significantly tolerated the decrease in compressive strength. The reason for this situation is that the polymer fibers strengthen the weak areas between the insoluble SF particles and the matrix. Due to the flexible structure of the polymer fibers, the formation of microcracks in the low-adhesion areas was limited. This situation also tolerated the decrease in compressive strength.

Increasing the SF ratio from 10% to 20% also caused a decrease in the compressive strength. Increasing the SF ratio from 10% to 20% in the fiber-free samples and basalt fiber samples decreased the compressive strength by 20% and 28%, respectively. In the sample using polymer fiber, the effect of increasing the SF ratio on the pressure reduction is limited. The reasons why increasing the SF ratio to 20% in the mixture decreases the compressive strength are similar to the reasons above. Especially, increasing the SF ratio to 20% in the mixture caused the insoluble SF particles in the matrix to increase even more. In this case, it caused a decrease in the compressive strength. Overall, as the SF ratio increased from $0\% \to 10\% \to 20\%$, the compressive strength decreased. This reduction is attributed to the increase in unreacted SF particles, micro-crack formation, decreased bonding gel formation, and increased porosity. Such adverse effects were determined to be lower in polymer fiber mixtures and higher in basalt fiber mixtures. This study reveals that even though the usage rate of SF is rising, optimizing the curing cycles and using a proper type of fiber can minimize the strength degradation. In previous literature studies, it has been stated that increasing the SF ratio in geopolymer concrete reduces the compressive strength [59,64,65]. Das et al. [58] reported that increasing the SF content in geopolymer concrete decreased the compressive strength, although it improved the slump value. Li et al. [66] stated that while there is an improvement in compressive strength when the SF ratio is used up to 10% in geopolymer concrete, the compressive strength decreases when SF is used at a rate greater than 10%. However, in this study, it is seen that the use of polymer fiber tolerates the negative effect of SF on compressive strength.

Among the samples without SF, the mixture without fiber reached the highest compressive strength, while among the samples containing 10% SF, the mixture with polymer fiber reached the highest compressive strength. Moreover, among the samples containing 20% SF, the use of polymer fiber significantly increased the compressive strength compared to other fiber types. Although basalt fibers have a high elasticity modulus, they cause fiber agglomeration and a weak interface despite their irregular distribution in the matrix, which causes a decrease in compressive strength. In addition, basalt fibers caused the formation of microvoids in the transition regions. However, due to the thermal expansion coefficient of basalt fibers being different from the matrix, it caused microcracks to form around the fibers, especially at an early age. For these reasons, basalt fiber addition can reduce the compressive strength instead of increasing it.



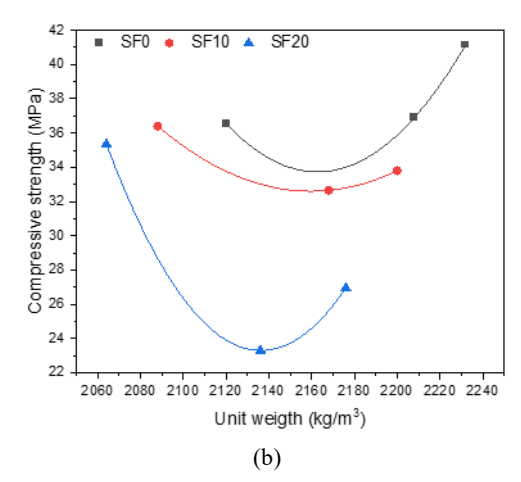


Fig. 9. (a) compressive strength and (b) relationship between compressive strength and unit weight of tested samples

The use of polymer fibers in geopolymer concrete improved the compressive strength. In addition, the polymer fibers had volumetric contributions due to their low specific gravity. In addition, due to the flexible structure of the polymer fibers, they exhibited a more homogeneous distribution in the matrix. Due to the more homogeneous distribution, a discontinuous environment was provided in the matrix. In addition, the microcracks around the polymer fibers were fewer than the basalt fibers. Thus, the local stresses around the polymer fibers were also limited. Moreover, the polymer fibers, especially in cases where the matrix weakens at high SF rates, maintain the structural integrity with the crack bridging effect and play a role in improving strength. Therefore, the SF20PF20 sample showed the highest strength in the entire SF20 group (35.35 MPa). The fiber-free samples recorded the highest compressive strength values in this group owing to the absence of weak points where fiber-matrix transition regions occur, particularly in the low SF ratios. On the other hand, with no mechanism to control cracking, its performance in resisting environmental effects may be curtailed. At low SF ratios, fiber-free mixtures gave the maximum value of compressive strength since the matrix is solid and homogeneous. On the other hand, the polymer fiber additive had an obvious stabilizing effect on the damaged matrix at high SF ratios and had a more favorable reaction than the basalt fiber additive. Despite the potential for high strength, basalt fibers can limit compressive strength due to dispersion issues and interfacial failure in the formulation. In such systems with high SF, polymer fiber must be preferred considering mix design, whereas an increase in distribution homogeneity and workability for basalt fiber must be achieved.

3.2.2. Flexural strength

The flexural strength results are presented in Fig. 10. Increasing the SF ratio caused a significant decrease in the flexural strength of the fiberless samples. Among the fibered samples, it was observed that increasing the SF ratio did not have a significant effect on the flexural strength. The flexural strength was high in basalt fibered samples. SF has a significant effect on the flexural behavior of geopolymer concretes, especially those cured at an early age. Among the fiberless samples, increasing the SF ratio caused a significant decrease in the flexural strength. For example, while the fiberless mixture with a 0% SF ratio had a flexural strength of 4.80 MPa, this value decreased to 3.39 MPa when the SF ratio increased to 20%. The reason for this situation can be explained by the limited reaction of SF in the 24 hours. SF (with a high specific surface and amorphous structure) is known to demonstrate high pozzolanic activity at the appropriate pH and temperature conditions, yet the applied curing of 4 h at 60°C was insufficient for the complete activation of SF, resulting in a higher amount of unresolved SF particles within the matrix. In the transition areas, having the excess

binder, which led to the formation of weak adhesion zones due to the appearance of microcracks and increased porosity of these transition regions, caused a descending effect on the flexural strength. However, the negative effect of SF was partially balanced in the fiber-added mixtures. The addition of basalt fiber to the mixture caused the negative effect of SF on the flexural strength to decrease. For example, while the basalt fiber mixture with 0% SF ratio showed a flexural strength of 7.00 MPa, this value was measured as 6.20 MPa in a similar mixture with a 20% SF ratio. The ability of basalt fibers to avoid microcrack propagation in the matrix and load distribution by the load-bearing fiber-matrix bridging mechanism, due to its high elasticity modulus (89 GPa) and high tensile strength (~4800 MPa), proves this fact. However, it is important to mention that based on the rigid structure of basalt fibers, in special conditions where there is no or not enough binding gel generated in the matrices, voids and fiber agglomeration might take place at the fiber-matrix interfaces. In the samples using polymer fibers, the effect of increasing the SF ratio on the flexural strength was reduced. Due to the low specific gravity and flexible structure properties of the polymer fibers, they were more homogeneously distributed in the matrix. Due to this homogeneous distribution, the weak areas at the fiber-matrix interface were fewer compared to the basalt fiber samples. Moreover, due to the flexible structure of the polymer fibers, the local stresses formed around the fibers were compensated. Since the local stresses were compensated by the polymer fibers, the local stress concentrations were reduced. The formation of microcracks was limited due to the decrease in these stresses. Therefore, the matrix continuity is satisfied. This mechanism contributed to the preservation of the flexural strength, especially in high-ratio mixtures where the binding capacity of the SF decreased.

The effect of using both basalt fiber and polymer fiber on the flexural strength is observed. Fibers played an active role in resisting tensile stresses, especially in the tensile region of the section. Crack development in the tensile region was limited. In addition, the bridging effect of fibers against cracks in the matrix was also effective on the flexural strength. Due to the bridging mechanism of fibers against cracks, the continuity of load transfer within the matrix was ensured. In this case, it prevented sudden and brittle fractures. The load-deflection curves of the samples under flexural moment are presented in Fig. 11. In particular, the significant effect of basalt fiber reinforcement on flexural performance is seen. It is seen that the loaddeflection curves of the samples consist of three regions. An elastic behavior is observed in the loaddeflection graphs of the samples in the first section. It is seen that the behavior in this region is independent of the material property and is related to the section rigidity. In addition, the slope of this section also provides information about the elastic modulus of the samples. This shows that the elasticity modulus of both basalt and polymer fiber samples is higher than the samples without fibers. In the second region, at the end of the elastic region, the graphs exhibit non-linear behavior instead of linear behavior. Although this behavior was observed in basalt fiber samples, it was not observed in fiberless and polymer fiber samples. The third region is the region where the strength decreases after the maximum load. In both fiberless and polymer fiber samples, a sudden loss of strength was observed after the maximum load was reached. However, in basalt fiber samples, the strength decreases after the maximum load is reached more gradually. However, the ductility of polymer fiber samples is higher than that of fiberless samples. Also, the images of samples after the flexural test are shown in Fig. 12.

In summary, both types of fiber can improve the flexural strength of SF-based geopolymer concrete, but they have different effects and mechanisms. Basalt fibers make a brilliant contribution to preventing crack development, owing to their high strength and rigidity, while polymer fibers limit the impact of microcracks with their flexibility and constant distribution ability, and maintain continuity in the matrix. With increasing SF ratio, the role of basalt fibers decreases slightly, with a high flexural strength maintained, while polymer fibers show stable performance under increasing porosity and weak binding conditions. In this sense, it has been concluded that fiber type and binding structure should be evaluated together in the design of the geopolymer concrete, and that polymer fibers may be more advantageous in systems with high rates of SF

use, and basalt fibers may be more productive in systems with less use. There are many studies in the literature reporting that fiber reinforcement increases the flexural strength in geopolymer concrete [67-69]. However, studies indicating that the effect of SF on the flexural strength is tolerated by the fibers are limited. In this study, it was concluded that the effect of SF on the flexural strength is tolerated by using both basalt and polymer fibers.

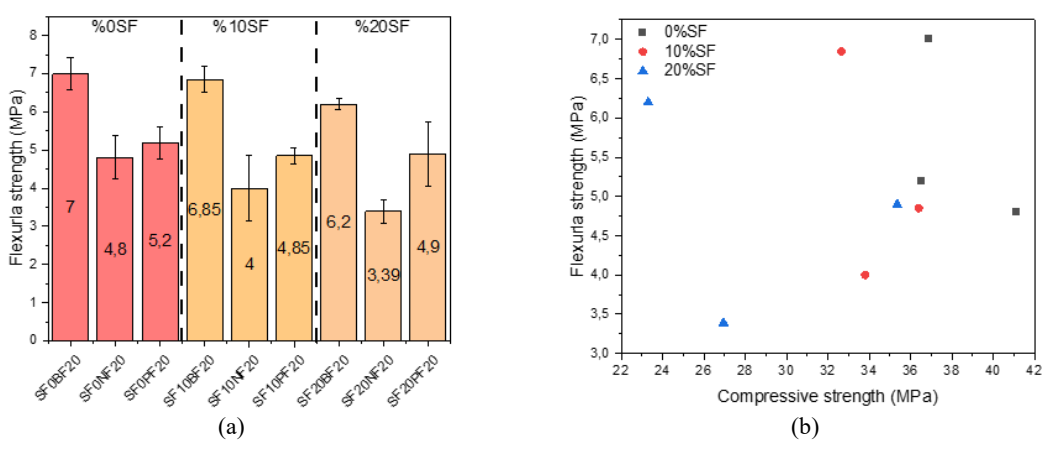


Fig. 10. (a) Flexural strength and (b) relationship between compressive strength and flexural strength of tested samples

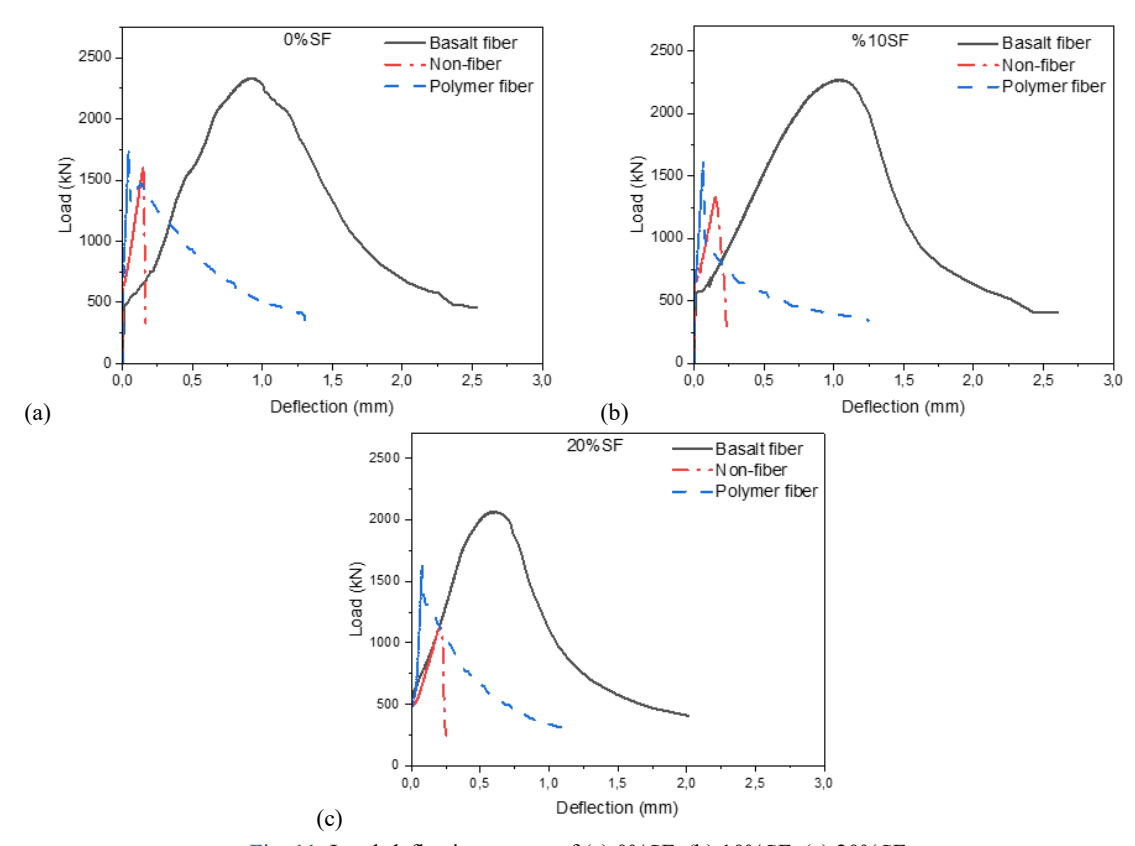


Fig. 11. Load-deflection curves of (a) 0%SF, (b) 10%SF, (c) 20%SF

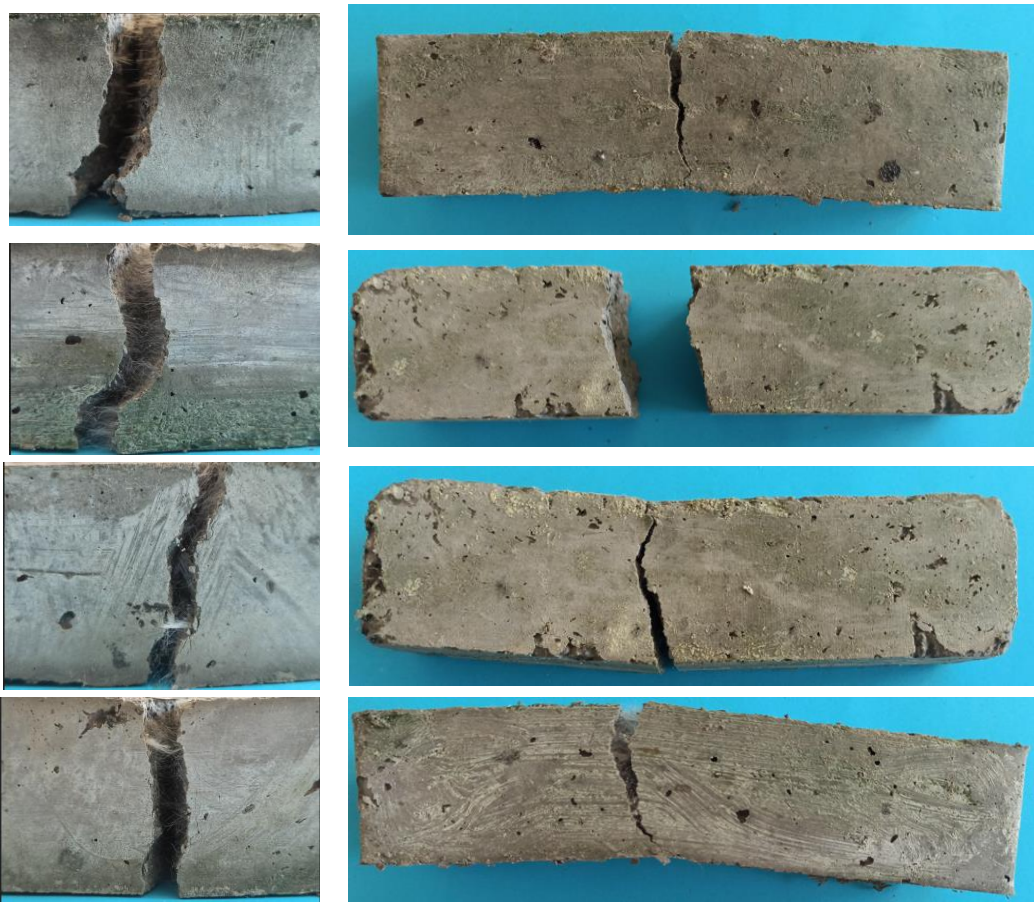


Fig. 12. Images of samples after the flexural test

3.3. High temperature effect

3.3.1. Compressive strength and mass loss after high temperature exposure

The compressive strength results of the samples after high temperature are presented in Fig. 13a. When the temperature exposed to the samples increased from 20°C to 100°C, the compressive strengths increased by 5%-25%. When the temperature to which the samples were exposed was increased to 100°C, the excess moisture in the sample evaporated, and the pores partially closed. This increased the compactness of the matrix and caused the strength to increase. Significant increases were also observed in the compressive strength of the fibrous samples. For example, the compressive strength of the SF0BF sample increased from 36.9 MPa to 42.5 MPa. The reason for this situation was that the fibers were better interlocked with the matrix at high temperatures.

By increasing the temperature to 100°C, alkali activators in the matrix reached more surfaces at the micro level and caused the geopolymerization process to progress better. In addition, especially due to the slow reaction feature and low reactivity of SF during the 24 hours, binding phases such as N-A-S-H and C-A-S-H were not fully formed. When the samples were exposed to 100°C, the solubility of Si⁴⁺ and Al³⁺ ions in SF and GBFS increased. The dissolved Si⁴⁺ and Al³⁺ ions reacted more effectively with Na⁺ ions and formed N-A-S-H gels. Due to the presence of GBFS, CaO reacted and formed C-A-S-H gels. These binding gels formed by the high temperature effect caused the filling of the voids in the matrix and the tightening of the internal structure. In this case, it caused an increase in compressive strength. Moreover, the temperature cure

applied to the samples for 4 hours at 60°C was not sufficient for the complete activation of SF. After the samples were exposed to a temperature of 100°C, this temperature created an additional curing effect on the samples. This second curing effect caused incomplete reactions in the matrix to progress. This situation created a reaction accelerator effect in the matrix. After the samples containing Na-silicate and GBFS were heated to 100°C, they may cause thermal contractions at the micro level. These thermal contractions prevented the formation of local stresses due to basalt fiber and polymer fiber. The formation of cracks was prevented in this way. The increase in the compressive strength of the samples produced from geopolymer concrete due to exposure to a temperature of 100°C is related to chemical and physical processes such as (i) decrease in the viscosity of the activators, (ii) better formation of binder gels during the geopolymerization process, (iii) development of the cure effect, instead of "water evaporation and pore closure" as in traditional concretes.

Increasing the temperature to 200°C causes the compressive strength increased, although the rate of the increase in compressive strength decreased. However, the compressive strength remained constant in some samples. Nevertheless, when compared to the compressive strength of the samples cured at 60°C, the compressive strength of the samples exposed to 200°C increased significantly. In this case, as explained above, this was due to the formation of more binder gel because of temperature. In the samples using polymer fibers, there was a slight loss of strength. The reason for this situation is that the temperature of 200°C is closer to the melting temperature of polymer fibers (255–265°C). For example, the compressive strength of the SF10PF20 sample decreased from 39.55 MPa to 38.65 MPa. In the samples with basalt fibers (for example, SF0BF20: 48.10 MPa), the strength reached its maximum value. This is due to the high temperature resistance of the basalt fibres (+950°C). Heat treatment up to 200°C represents the optimum resistance level, especially for mixtures with basalt fibres and low SF content. However, the effect of the polymer fibres remains stable or begins to weaken at this point.

As the temperature increased to 400°C, a significant decrease in the compressive strength of all samples occurred between 40% and 75%. This temperature value significantly affected the strength limits of both the matrix and the fibers. Cracks, thermal expansion differences, and deterioration of the binder phase are intensely seen in the geopolymer matrix. This is the main reason for the loss of strength. It was observed that the greatest decrease was experienced in basalt fiber mixtures. This situation may be due to the deterioration of the compatibility of the basalt fibers with the matrix due to the thermal expansion difference. In mixtures with a high SF ratio (especially SF20), the decrease in strength is at higher levels. Because the binding was insufficient at the beginning, the weak areas completely deteriorated at 400°C. For example, the compressive strength of the SF20BF20 sample decreased from 34.0 MPa to 9.75 MPa. After 400°C, serious strength losses occurred due to both the deterioration of the binder gel structures and fiber-matrix incompatibilities. The fiber type and SF ratio directly affect the severity of this decrease. The least loss was observed in samples SF10PF20 and SF20PF20, reflecting the positive effect of the flexibility of polymer fibers and the optimum selection of the SF ratio. Tayeh et al. [70] also stated that geopolymer concrete exposed to 100°C and 200°C temperatures increased its compressive strength. Studies in the literature also reported that applying temperatures up to 300°C to geopolymer concrete improved its compressive strength [71, 72]. Additionally, studies in the literature have shown that exposure of geopolymer concrete to a temperature of 400°C significantly reduced its compressive strength [73-75].

The change in the masses of the samples after the high temperature effect is presented in Fig. 13b. Although the masses of the samples exposed to 100°C and 200°C increased, the masses of the samples exposed to 400°C decreased. The highest mass increase and the highest mass decrease were reached in the SF0PF20 and SF20BF20 samples, respectively. Since NaOH and especially Na₂SiO₃ are hygroscopic compounds that can absorb moisture from the air, the active alkaline components remaining in the samples contribute to gelation by absorbing atmospheric moisture from the environment during the heating process

up to 100°C. This may cause a small net mass increase due to water absorption of the solid components participating in the reaction. Since the dissolution and polycondensation reactions are even faster at 200°C, the mass increase occurred due to the formation of N-A-S-H and C-A-S-H gels continuing. After the samples were exposed to 400°C, a mass loss of 5%-10% occurred. Especially at 400°C, the structure of the binder gels was significantly broken down. Overheated NaOH/Na₂SiO₃ residues could evaporate. This situation caused mass loss. Aslani and Asif [71] and Verna et al. [76] also reported that the exposure of geopolymer concrete to temperatures of 100°C and 200°C caused an increase in mass parallel to the results of this study. Moreover, Verna et al. [76] reported that the exposure of geopolymer concrete to 400°C caused its mass to decrease.

In the temperatures between 100–200°C, the mass change rates were positive, which is attributed to the hygroscopic effect of the sodium silicate and sodium hydroxide activated materials, contrary to the conventional water evaporation effect. The increased net mass of the samples was due to the retaining ability of the binder gel structures obtained at those temperatures, and particularly the thermal expansion tendency of the polymeric fibers. Conversely, the significant mass loss encountered in all samples at 400°C relates to the decomposition of the binder phases, thermal separations, and fiber/matrix interface deteriorations.

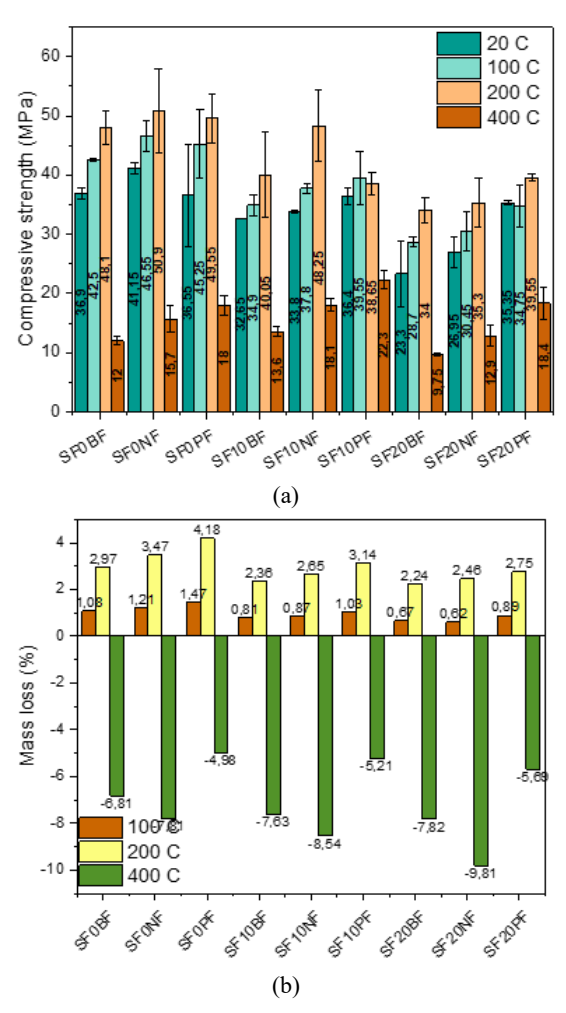


Fig. 13. (a) Compressive strength results and (b) mass loss of tested samples after high temperature exposure

3.3.2. Flexural strength after high temperature exposure

The flexural strength results of the samples exposed to high temperatures are presented in Table 5, and the load-deflection curves in Figs. 14-16. The flexural strength of most of the samples exposed to 100°C increased. Although the increasing trend in the flexural strength of the samples exposed to 200°C continued, the flexural strength of the samples exposed to 400°C decreased. The exposure of the samples to 100°C caused the geopolymerization process to progress and the N-A-S-H and C-A-S-H gels to develop better. For this reason, the matrix became more compact, and the fiber-matrix interaction increased. Moreover, the crack-bridging effect of the polymer and basalt fibers in the matrix became more effective. Due to the bridging effect of the fibers, the internal stresses of the matrix decreased, and the load transfer became continuous. The significant increase seen in the SF0 group is related to the more reactive binder phase production of the mixtures without SF.

The matrix exhibited more rigid behavior due to the samples being exposed to a temperature of 200°C (Fig. 17). However, in some samples (especially those with polymer fibers), the fiber-matrix interface was negatively affected by this situation due to the fibers starting to be affected by the temperature. At 200°C, the flexural strength generally reached its peak or remained stable. However, for mixtures containing a high SF ratio and polymer fibers, the flexural strength started to decrease. At this point, the type of fiber and the SF ratio are the main factors determining the performance. The flexural strength of all samples exposed to a temperature of 400°C decreased significantly. At this temperature, the flexural strength decreased due to significant damage to both the fibers and the matrix. At a temperature of 400°C, the N-A-S-H and C-A-S-H binder gels in the matrix were significantly damaged. After 400°C, regardless of the fiber type, the flexural strength decreased significantly because the microstructure was damaged. The load carrying capacity decreases, and the crack propagation becomes uncontrollable.

Soaking in high temperature (at 60°C and 70°C) has a greater effect on flexural strength than soaking in lower temperature (at 20°C and 40°C). The development of gelation in the matrix at 100°C, the interlocking of the fibers in the matrix, and the decline of internal stresses contributed to a significant increase in flexural strength. Flexural strength was maximized in some mixtures at 200°C. The binding phases reaching the maximum reaction level at this temperature were successful. On the contrary, at 400°C, the flexural strength of all the mixtures decreased significantly due to the microstructure destruction, gel disintegration, and loss of function of the fibers. The basic parameters defining the severity of this decrease were the SF ratio and fiber type.

Table 5. Flexural s	strength of tested	l samples after hi	gh temperature	(MPa)

		• •	·	
Specimen	20°C	100°C	200°C	400°C
SF0BF20	7.00	7.15	6.60	3.11
SF0NF20	4.80	5.15	5.35	2.25
SF0PF20	5.20	5.10	5.65	2.85
SF10BF20	6.85	6.95	5.95	3.81
SF10NF20	4.00	4.15	3.81	1.95
SF10PF20	4.85	4.40	5.22	3.00
SF20BF20	6.20	6.50	5.93	3.25
SF20NF20	3.39	3.85	3.35	1.90
SF20PF20	4.90	4.85	5.13	2.75

Alcan Alcan

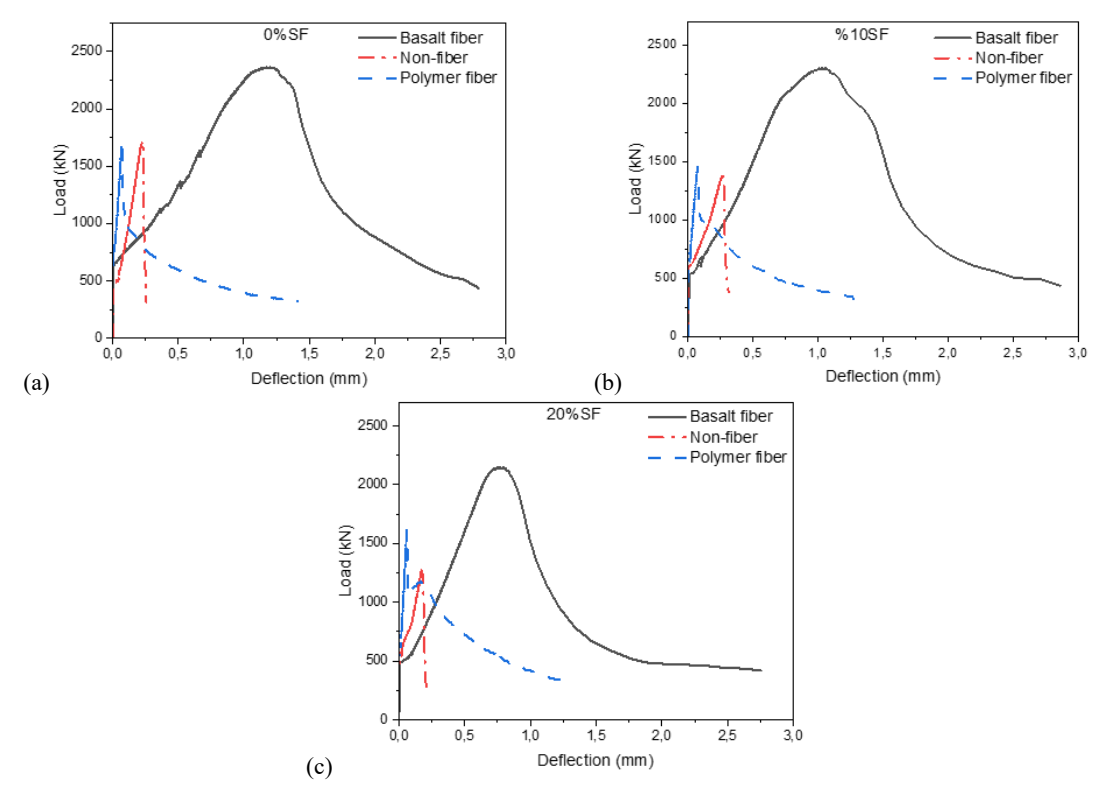


Fig. 14. Load-deflection curves of tested beams after 100°C exposure (a) 0% SF, (b) 10%SF, (c) 20% SF

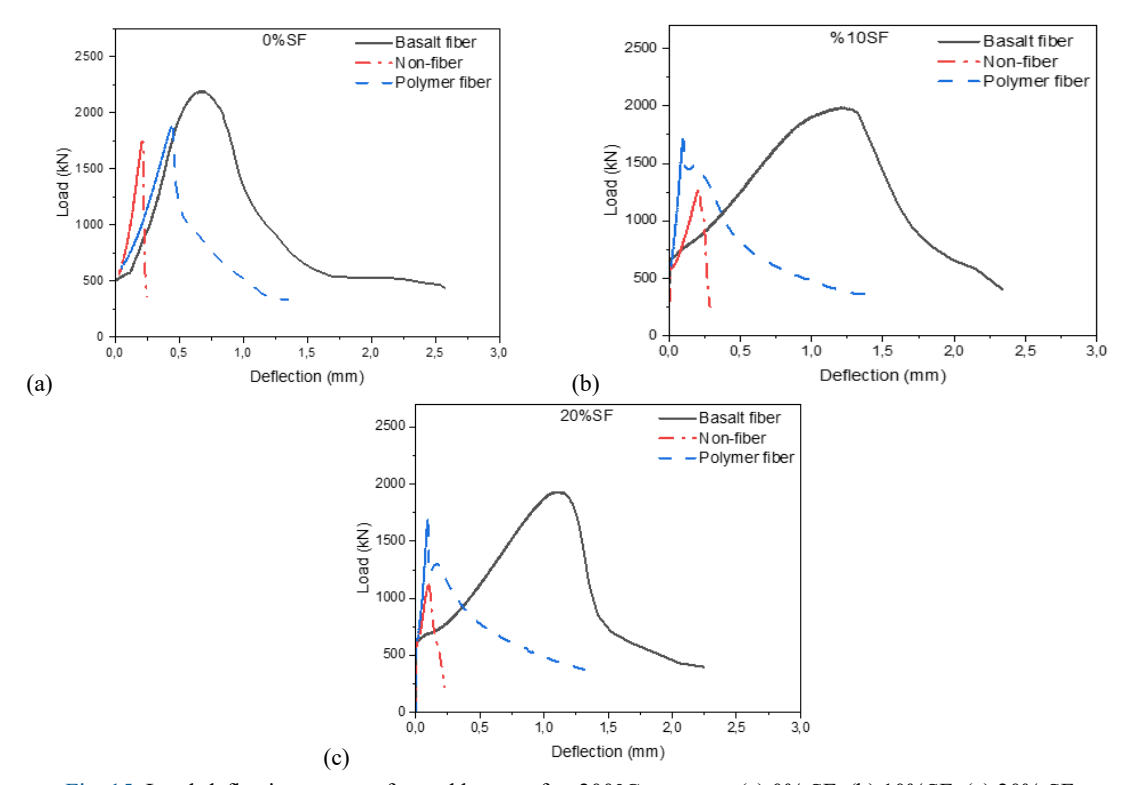


Fig. 15. Load-deflection curves of tested beams after 200°C exposure (a) 0% SF, (b) 10%SF, (c) 20% SF

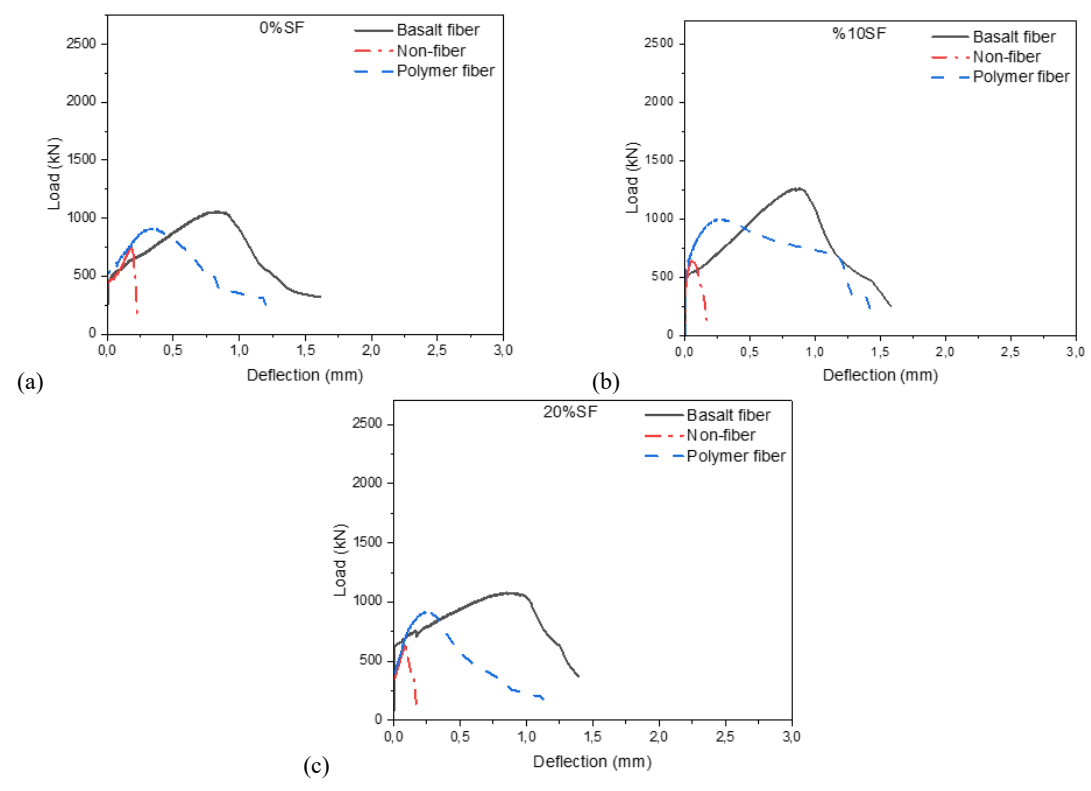


Fig. 16. Load-deflection curves of tested beams after 400°C exposure (a) 0% SF, (b) 10%SF, (c) 20% SF

The load-deflection curves of the samples exposed to high temperatures were also similar to the graphs of the samples kept in normal environments. It is seen that basalt fibers play an active role among the samples exposed to high temperatures. It is seen that the basalt fiber samples exhibit more ductile behavior. The samples with and without polymer fibers exhibited a sudden decrease in strength after reaching the maximum load. Although there was a decrease in the load carrying capacity as the temperature value to which the samples were exposed increased to 100°C and 200°C, there was no significant decrease in the deformation capacity. However, significant decreases occurred in both the load-carrying capacity and deformation capacity of the samples exposed to 400°C. Although the load carrying capacities of the samples with and without polymer fibers were almost the same in the samples exposed to 100°C, the deformation capacity of the samples with polymer fibers was higher. For this reason, the samples with polymer fibers exhibited more ductile behavior compared to the samples without fibers. A more ductile behavior was exhibited due to the effectiveness of polymer fibers in the matrix. It is observed that the use of basalt fibers in samples exposed to 200°C also caused more ductile behavior. Due to the resistance of basalt fibers to high temperatures, these samples exhibited more ductile behavior compared to other samples. Among these samples, the use of polymer fibers exhibited more ductile behavior compared to samples without fibers. Both the load-carrying capacity and deformation capacity of samples with polymer fibers are higher than samples without fibers. Crack distribution was prevented due to the bridging effect of fibers in the matrix. Significant decreases occurred in both the load-carrying capacity and deformation capacity of samples exposed to 400°C. In particular, the load-carrying capacity and deformation capacity of samples without fibers decreased significantly. Among these samples, the load-carrying capacity of samples with polymer fibers is almost the same as the deformation capacity of samples with basalt fibers. A positive effect of using polymer fibers on the load-deflection curves at a temperature of 400°C was observed.

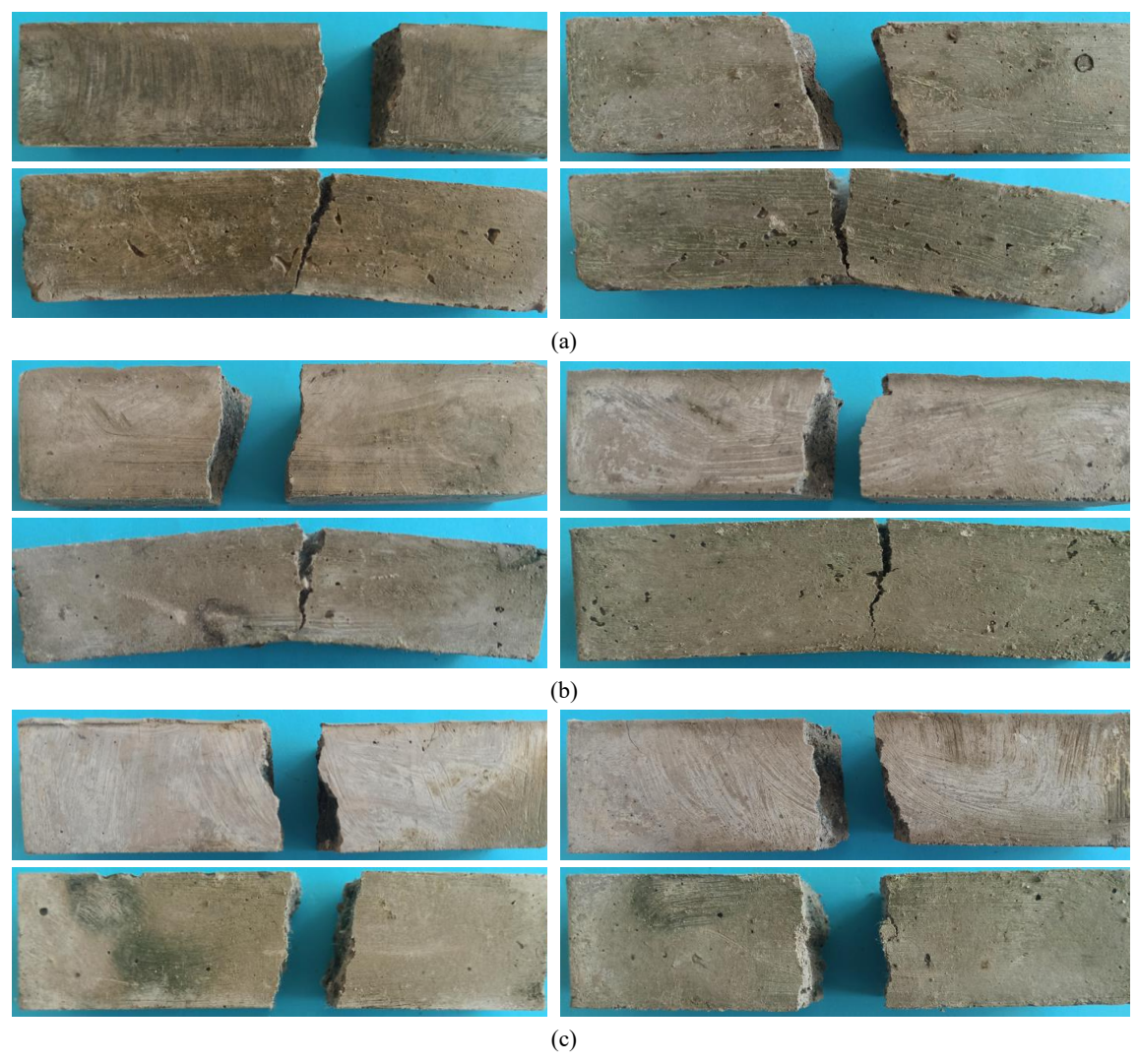


Fig. 17. Images of samples exposed to high temperatures after flexural test (a) 100°C, (b) 200°C, (c) 400°C

4. Conclusions

The aim of this study is to experimentally investigate the effects of using SF at different rates (0%, 10% and 20%) instead of GBFS in geopolymer concrete mixture and two different fiber types (basalt fiber and polymer fiber) on mechanical strength, physical properties, and thermal performance. Dry unit weight and water absorption rate tests were applied for physical properties, in which the compressive strength and flexural strength tests were applied for mechanical strength. Furthermore, compressive strength, flexural strength, and mass loss of samples exposed to 100°C, 200°C, and 400°C temperatures were evaluated for thermal performance. The findings are summarized below:

• The increase in SF ratio in the geopolymer concrete mixture caused the compressive strength to decrease. Since SF limits the formation of the binding gel in the matrix at 24 hours of early age, a negative effect of SF on the early age compressive strength was determined. This effect was associated with the insufficient activation of SF and the formation of micro-voids by the particles remaining undissolved in the matrix.

- In samples exposed to 100°C, compressive strength increased by up to 25% compared to the initial temperature (20°C). In particular, in the SF0BF sample, the compressive strength increased by approximately 15%, from 36.9 MPa to 42.5 MPa.
- The use of basalt and polymer fibers in the geopolymer mixture has balanced the negative effect of SF on mechanical performance. The formation and propagation of microcracks have been limited due to the low specific gravity, flexible structure, and homogeneous distribution of polymer fibers in the matrix. This has also caused an improvement in the mechanical strength. However, the high elasticity modulus of basalt fibers has increased the flexural performance. Nevertheless, the irregular distribution of basalt fibers in the matrix has also caused the compressive strength to decrease.
- The exposure of the samples to 100°C temperature positively affected both the flexural strength and the compressive strength. After 100°C, the flexural strength and compressive strength increased. This increase can be explained by the development of gel formation, decreased porosity, and increased effectiveness of the activators due to the effect of temperature as a second cure. However, after 400°C, significant decreases were observed in the compressive strength of all samples.
- The compressive strength of the SF20BF sample decreased by 71% after 400°C. A significant decrease in compressive strength occurred due to the high temperature caused by both the high SF ratio and the defective regions at the fiber-matrix interface.
- The synergy between silica fume and fiber types enabled a balanced improvement in both mechanical strength and thermal durability. While a certain decrease in the strength values of the samples was observed as the SF ratio increased, the fibers compensated for the early age weaknesses by limiting microcracks. In addition, fibers further improved flexural strength and ductility, highlighting the complementary roles of mechanical and physical enhancements in geopolymer concrete.

Future research could examine the long-term durability of geopolymer concrete under thermal cycling. Optimizing curing conditions to improve early-age SF reactivity and developing better fiber dispersion methods to prevent agglomeration are also important. Studies on hybrid fiber use and varying fiber volumes may offer further performance enhancements.

Conflict of interest

The author declares that he has no known competing financial interests or personal relationships that could have appeared to influence the work reported in this paper.

Funding

This research received no external funding.

Data availability statement

Data generated during the current study are available from the corresponding author upon reasonable request.

References

- [1] Abdulhaleem KN, Hamada HM, Osman AI, Yousif ST, Humada AM, Majdi A (2025) A comprehensive review of sustainable geopolymer concrete using palm oil clinker: Environmental and engineering aspects. Energy Science Engineering 13:958–979. https://doi.org/10.1002/ese3.1977
- [2] Al-Tam SM, Riad A, Mohammed N, Al-Otaibi A, Youssf O (2025) A comprehensive assessment of sustainable high-strength hybrid geopolymer concrete. Results in Engineering 104613. https://doi.org/10.1016/j.rineng.2025.104613

[3] Oluwafemi J, Ofuyatan O, Adedeji A, Bankole D, Bitrus V (2025) Investigation of optimum alkaline activator ratio and geopolymerization rate of cattle bone ash-based geopolymer concrete. Case Studies in Construction Materials e04526. https://doi.org/10.1016/j.cscm.2025.e04526

- [4] Rathee M, Singh N (2024) Reviewing geopolymer concrete: a possible sustainable structural material of future. Environment, Development Sustainability. https://doi.org/10.1007/s10668-024-05526-0
- [5] Zargaleh MRA, Mazloom M, Samimi MJ, Ramesht MH (2025) The effect of replacing GGBFS with fly ash on the fracture parameters of geopolymer concrete. Materials Letters 138394. https://doi.org/10.1016/j.matlet.2025.138394
- [6] Metwally GA, Elemam WE, Mahdy M, Ghannam M (2025) A comprehensive review of metakaolin-based ultrahigh-performance geopolymer concrete enhanced with waste material additives. Journal of Building Engineering 112019. https://doi.org/10.1016/j.jobe.2025.112019
- [7] Panda S, Nanda A, Panigrahi SK (2024) Potential utilization of waste plastic in sustainable geopolymer concrete production: A review. Journal of Environmental Management 366:121705. https://doi.org/10.1016/j.jenvman.2024.121705
- [8] Sharma U, Gupta N, Bahrami A, Özkılıç YO, Verma M, Berwal P, Althaqafi E, Khan MA, Islam S (2024) Behavior of fibers in geopolymer concrete: A comprehensive review. Buildings 14(1):136. https://doi.org/10.3390/buildings14010136
- [9] Arab MAES, Mohamed AS, Taha MK, Nasr A (2025) Microstructure, durability and mechanical properties of high strength geopolymer concrete containing calcinated nano-silica fume/nano-alumina blend. Construction Building Materials 472:140903. https://doi.org/10.1016/j.conbuildmat.2025.140903
- [10] Song P, Liu Y, Kong L, Tang Z, Sun G (2025) Research on design and optimization for compositions of ultra-high performance geopolymer concrete. Journal of Building Engineering 100:111750. https://doi.org/10.1016/j.jobe.2024.111750
- [11] Yanting M, Bo D, Xiaotong Y, Da C, Yingdi L (2025) Study on mechanical properties and durability of geopolymer concrete with oyster shell aggregate. Construction Building Materials 472:140926. https://doi.org/10.1016/j.conbuildmat.2025.140926
- [12] Al-Naghi AAA, Ghazouani N, Selmi A, Alashker Y, Raza A (2025) Combined effects of elevated temperature, sulfates and chlorides on performance of fly ash and metakaolin-based recycled aggregate geopolymer concrete. Journal of Building Engineering 99:111561. https://doi.org/10.1016/j.jobe.2024.111561
- [13] Hamada HM, Al-Attar A, Beddu S, Askar MK, Yousif ST, Majdi A (2025) Impact of rice husk ash on geopolymer concrete: A literature review and future directions. Case Studies in Construction Materials e04476. https://doi.org/10.1016/j.cscm.2025.e04476
- [14] Thatikonda N, Mallik M, Rao SV, Dubey S (2025) Performance and microstructural characterization of sustainable self-compacting geopolymer concrete with multi-component binders. Sustainable Chemistry Pharmacy 44:101926. https://doi.org/10.1016/j.scp.2025.101926
- [15] Beiraghi H, Doostmohammadi MR (2025) Effect of metakaolin and microsilica on the mechanical behavior of slag-based geopolymer concrete containing PP fibers. Innovative Infrastructure Solutions 10(3):1-14. https://doi.org/10.1007/s41062-025-01904-3
- [16] Feng Z, Zhang P, Guo J, Zheng Y, Hu S (2025) Single and synergistic effects of nano-SiO₂ and hybrid fiber on rheological property and compressive strength of geopolymer concrete. Construction Building Materials 472:140945. https://doi.org/10.1016/j.conbuildmat.2025.140945
- [17] Hassan A, Zhang C (2025) Dynamic and static behaviour of geopolymer concrete for sustainable infrastructure development: Prospects, challenges, and performance review. Composite Structures 118984. https://doi.org/10.1016/j.compstruct.2025.118984
- [18] Heshmati M, Sheikh MN, Hadi M (2025) A comprehensive review of the fresh and hardened characteristics of self-compacting geopolymer concrete. Journal of Sustainable Cement-Based Materials 14(4):816–835. https://doi.org/10.1080/21650373.2025.2461182
- [19] Rihan MAM, Alahmari TS (2025) Review of recent development regarding strength, durability, and microstructure properties of geopolymer concrete containing rice husk ash. Advances in Civil Engineering 2025(1):7211661. https://doi.org/10.1155/adce/7211661

- [20] Srikrishna TC, Noolu V, Sudheer Kumar Reddy B, Alaneme GU, Prasad RD, VishnuPriyan M (2025) Investigations on mechanical and stress strain characteristics of geopolymer concrete reinforced with glass fibers. Scientific Reports 15(1):6335. https://doi.org/10.1038/s41598-025-90752-3
- [21] Kalifa P, Chene G, Galle C (2001) High-temperature behaviour of HPC with polypropylene fibres: From spalling to microstructure. Cement Concrete Research 31(10):1487-1499. https://doi.org/10.1016/S0008-8846(01)00596-8
- [22] Lahoti M, Tan KH, Yang EH (2019) A critical review of geopolymer properties for structural fire-resistance applications. Construction Building Materials 221:514-526. https://doi.org/10.1016/j.conbuildmat.2019.06.076
- [23] Eltantawi I, Sheikh MN, Hadi MN (2025) Influence of stainless steel fibres on the mechanical properties of self-compacting ultra-high performance geopolymer concrete. Construction Building Materials 463:140092. https://doi.org/10.1016/j.conbuildmat.2025.140092
- [24] HM AK, Shoba M (2025) Durability and microstructure of fiber-reinforced geopolymer concrete with FA and GGBS. Structures 71:108096. https://doi.org/10.1016/j.istruc.2024.108096
- [25] Wang W, Zhang P, Dai X, Zheng Y, Hu S (2025) Workability of self-compacting geopolymer concrete: The effect of nano-SiO₂ and steel-polyvinyl alcohol hybrid fiber. Construction Building Materials 460:139849. https://doi.org/10.1016/j.conbuildmat.2024.139849
- [26] Özdemir MHS, Bayrak B, Aydın AC (2025) Bond performance of geopolymer concrete with basalt/glass fiber under elevated temperature. Engineering Structures 324:119368. https://doi.org/10.1016/j.engstruct.2024.119368
- [27] Sangi R, Bollapragada SS (2024) A comparative study: impact of fibers on the interfacial shear strength of geopolymer concrete. Slovak Journal of Civil Engineering 32(4):60-67. https://doi.org/10.2478/sjce-2024-0026
- [28] Zhang P, Feng Z, Guo J, Zheng Y, Yuan P (2024) Mechanical behavior and microscopic damage mechanism of hybrid fiber-reinforced geopolymer concrete at elevated temperature. Ceramics International 50(24):53851-53866. https://doi.org/10.1016/j.ceramint.2024.10.238
- [29] Min Wl, Jin Wl, He Xy, Wu Rj, Chen Ky, Chen Jj, Xia J (2024) Experimental study on the flexural fatigue performance of slag/fly ash geopolymer concrete reinforced with modified basalt and PVA hybrid fibers. Journal of Building Engineering 94:109917. https://doi.org/10.1016/j.jobe.2024.109917
- [30] Mohammed ADAA, Ronghui W, Huseien GF (2024) Mechanical properties of natural jute fiber-reinforced geopolymer concrete: effects of various lengths and volume fractions. Journal of Composites Science 8(11):450. https://doi.org/10.3390/jcs8110450
- [31] Nikmehr B, Kafle B, Al Zand AW, Al-Ameri R (2024) The effect of hybrid basalt fibres on the mechanical and structural characteristics of geopolymer concrete containing geopolymer-coated recycled concrete aggregates. Construction Building Materials 450:138649. https://doi.org/10.1016/j.conbuildmat.2024.138649
- [32] Chen P, Li Y, Yin L, Wang Z (2024) Review on mechanical properties of fiber-reinforced geopolymer concrete after high-temperature exposure. Iranian Journal of Science Technology, Transactions of Civil Engineering 48(6):3829-3851. https://doi.org/10.1007/s40996-024-01347-3
- [33] Liu Y, Hu X, Du Y, Nematollahi B, Shi C (2024) A review on high-temperature resistance of geopolymer concrete. Journal of Building Engineering 111241. https://doi.org/10.1016/j.jobe.2024.111241
- [34] Manzoor T, Bhat JA, Shah AH (2024) Performance of geopolymer concrete at elevated temperature— A critical review. Construction Building Materials 420:135578. https://doi.org/10.1016/j.conbuildmat.2024.135578
- [35] Yang H, Li H, Jiang J (2024) Predictive modeling of compressive strength of geopolymer concrete before and after high temperature applying machine learning algorithms. Structural Concrete. https://doi.org/10.1002/suco.202400552
- [36] Abd Ellatief M, Abadel AA, Federowicz K, Abd Elrahman M (2023) Mechanical properties, high temperature resistance and microstructure of eco-friendly ultra-high performance geopolymer concrete: Role of ceramic waste addition. Construction Building Materials 401:132677. https://doi.org/10.1016/j.conbuildmat.2023.132677
- [37] Dalgıç A, Yılmazer Polat B (2024) The behavior of ceramic fiber geopolymer concrete under the effect of high temperature. Applied Sciences 14(4):1607. https://doi.org/10.3390/app14041607
- [38] Rahjoo M, Goracci G, Gaitero JJ, Martauz P, Rojas E, Dolado JS (2022) Thermal energy storage (TES) prototype based on geopolymer concrete for high-temperature applications. Materials 15(20):7086. https://doi.org/10.3390/ma15207086

[39] Rahjoo M, Goracci G, Martauz P, Rojas E, Dolado JS (2022) Geopolymer concrete performance study for high-temperature thermal energy storage (TES) applications. Sustainability 14(3):1937. https://doi.org/10.3390/su14031937

- [40] Tahwia AM, Abd Ellatief M, Bassioni G, Heniegal AM, Abd Elrahman M (2023) Influence of high temperature exposure on compressive strength and microstructure of ultra-high performance geopolymer concrete with waste glass and ceramic. Journal of Materials Research Technology 23:5681-5697. https://doi.org/10.1016/j.jmrt.2023.02.177
- [41] Wang Z, Fu C, Wang K, Zhao J, Shumuye ED, Yang Z (2024) Effect of geopolymer concrete cover on improving tensile and transverse shear behaviors of BFRP bars after exposure to high temperature. Case Studies in Construction Materials 20: e02862. https://doi.org/10.1016/j.cscm.2024.e02862
- [42] Zhong W, Ding H, Zhao X, Fan L (2023) Mechanical properties prediction of geopolymer concrete subjected to high temperature by BP neural network. Construction Building Materials 409:133780. https://doi.org/10.1016/j.conbuildmat.2023.133780
- [43] Paruthi S, Rahman I, Husain A, Khan AH, Manea-Saghin AM, Sabi E (2023) A comprehensive review of nano materials in geopolymer concrete: Impact on properties and performance. Developments in the Built Environment 16:100287. https://doi.org/10.1016/j.dibe.2023.100287
- [44] Tanyildizi H, Yonar Y (2016) Mechanical properties of geopolymer concrete containing polyvinyl alcohol fiber exposed to high temperature. Construction Building Materials 126:381-387. https://doi.org/10.1016/j.conbuildmat.2016.09.001
- [45] Zaid O, Sor NAH, Martínez-García R, de Prado-Gil J, Elhadi KM, Yosri AM (2024) Sustainability evaluation, engineering properties and challenges relevant to geopolymer concrete modified with different nanomaterials: A systematic review. Ain Shams Engineering Journal 15(2):102373. https://doi.org/10.1016/j.asej.2023.102373
- [46] Zhang H, Li L, Yuan C, Wang Q, Sarker PK, Shi X (2020) Deterioration of ambient-cured and heat-cured fly ash geopolymer concrete by high temperature exposure and prediction of its residual compressive strength. Construction Building Materials 262:120924. https://doi.org/10.1016/j.conbuildmat.2020.120924
- [47] ASTM, ASTM-C-618 Standard Specification for Coal Fly Ash and Raw or Calcined Natural Pozzolan for Use. Annu, West Conshohocken, PA, 2012.
- [48] Alcan HG, Benli A, Öz A, Bayrak B, Kaplan G, Aydın AC (2024) Effective utilization of silica fume and waste colemanite in eco-sustainable prepacked geopolymers. Construction Building Materials 457:139438. https://doi.org/10.1016/j.conbuildmat.2024.139438
- [49] Alcan HG, Dheyaaldin MH, Toklu K, Bayrak B, Kaplan G, Aydın AC (2024) Effect of quaternary binder slag-based geopolymer slurries on mechanical durability and microstructural properties of green prepacked composites. Construction Building Materials 450:138571. https://doi.org/10.1016/j.conbuildmat.2024.138571
- [50] Bayrak B, Alcan HG, Özelmacı Durmaz ÖÇ, İpek S, Kaplan G, Güneyisi E, Aydın AC (2024) Studying the metakaolin content, fiber type, and high-temperature effects on the physico-mechanical properties of fly ash-based geopolymer composites. Archives of Civil Mechanical Engineering 25(1):2. https://doi.org/10.1007/s43452-024-01071-9
- [51] Alcan HG, Bayrak B, Öz A, Çelebi O, Kaplan G, Aydın AC (2024) Synergetic effect of fibers on geopolymers: Cost-effective and sustainable perspective. Construction Building Materials 414:135059. https://doi.org/10.1016/j.conbuildmat.2024.135059
- [52] Bayrak B, Alcan HG, Tanyıldızı M, Kaplan G, İpek S, Aydın AC, Güneyisi E (2024) Effects of silica fume and rice husk ash contents on engineering properties and high-temperature resistance of slag-based prepacked geopolymers. Journal of Building Engineering 92:109746. https://doi.org/10.1016/j.jobe.2024.109746
- [53] Bayrak B, Benli A, Alcan HG, Çelebi O, Kaplan G, Aydın AC (2023) Recycling of waste marble powder and waste colemanite in ternary-blended green geopolymer composites: mechanical, durability and microstructural properties. Journal of Building Engineering 73:106661. https://doi.org/10.1016/j.jobe.2023.106661
- [54] ASTM, ASTM C348–19 Standard Test Method for Flexural Strength of Hydraulic-Cement Mortars. ASTM International, West Conshohocken, PA, 2019.
- [55] ASTM, ASTM C349–18 Standard Test Method for Compressive Strength of Hydraulic-Cement Mortars (Using Portions of Prisms Broken in Flexure). ASTM International, West Conshohocken, PA, 2018.

- [56] ASTM, ASTM C642–13 Standard Test Method for Density, Absorption, and Voids in Hardened Concrete. ASTM International, West Conshohocken, PA, 2013.
- [57] Sevinç AH, Durgun MY (2020) Properties of high-calcium fly ash-based geopolymer concretes improved with high-silica sources. Construction Building Materials 261:120014. https://doi.org/10.1016/j.conbuildmat.2020.120014
- [58] Das SK, Mustakim SM, Adesina A, Mishra J, Alomayri TS, Assaedi HS, Kaze CR (2020) Fresh, strength and microstructure properties of geopolymer concrete incorporating lime and silica fume as replacement of fly ash. Journal of Building Engineering 32:101780. https://doi.org/10.1016/j.jobe.2020.101780
- [59] Pan Z, Tan M, Zheng G, Wei L, Tao Z, Hao Y (2024) Effect of silica fume type on rheology and compressive strength of geopolymer mortar. Construction Building Materials 430:136488. https://doi.org/10.1016/j.conbuildmat.2024.136488
- [60] Shariati M, Shariati A, Trung NT, Shoaei P, Ameri F, Bahrami N, Zamanabadi SN (2021) Alkali-activated slag (AAS) paste: Correlation between durability and microstructural characteristics. Construction Building Materials 267:120886. https://doi.org/10.1016/j.conbuildmat.2020.120886
- [61] Rukzon S, Rungruang S, Chaisakulkiet U, Posi P, Chindaprasirt P (2025) Strength, pore and corrosion characteristics of ceramic insulator powder-silica fume based ternary blended mortar. Cleaner Materials 15:100284. https://doi.org/10.1016/j.clema.2024.100284
- [62] Abdulhadi M, Haruna SI (2021) Experimental study on the rate of absorption of water of basalt, polypropylene, and steel fibers reinforced concrete. The Civil Engineering Journal 30(2):31. https://doi.org/10.14311/CEJ.2021.02.0036
- [63] Li Y, Wang Q, Xu S, Song Q (2023) Study of eco-friendly fabricated hydrophobic concrete containing basalt fiber with good durability, Journal of Building Engineering 65:105759. https://doi.org/10.1016/j.jobe.2022.105759
- [64] Liu Y, Shi C, Zhang Z, Li N, Shi D (2020) Mechanical and fracture properties of ultra-high performance geopolymer concrete: Effects of steel fiber and silica fume. Cement Concrete Composites 112:103665. https://doi.org/10.1016/j.cemconcomp.2020.103665
- [65] Wang F, Sun X, Tao Z, Pan Z (2022) Effect of silica fume on compressive strength of ultra-high-performance concrete made of calcium aluminate cement/fly ash based geopolymer. Journal of Building Engineering 62:105398. https://doi.org/10.1016/j.jobe.2022.105398
- [66] Li B, Gao A, Li Y, Xiao H, Chen N, Xia D, Wang S, Li C (2023) Effect of silica fume content on the mechanical strengths, compressive stress–strain behavior and microstructures of geopolymeric recycled aggregate concrete. Construction Building Materials 384:131417. https://doi.org/10.1016/j.conbuildmat.2023.131417
- [67] Noushini A, Hastings M, Castel A, Aslani F (2018) Mechanical and flexural performance of synthetic fibre reinforced geopolymer concrete. Construction Building Materials 186:54-475. https://doi.org/10.1016/j.conbuildmat.2018.07.110
- [68] Sathish Kumar V, Ganesan N, Indira PV, Murali G, Vatin NI (2022) Flexural behaviour of hybrid fibre-reinforced ternary blend geopolymer concrete beams. Sustainability 14(10):5954. https://doi.org/10.3390/su14105954
- [69] Zuaiter M, El-Hassan H, El-Maaddawy T, El-Ariss B (2023) Flexural and shear performance of geopolymer concrete reinforced with hybrid glass fibers. Journal of Building Engineering 72:106580. https://doi.org/10.1016/j.jobe.2023.106580
- [70] Tayeh BA, Zeyad AM, Agwa IS, Amin M (2021) Effect of elevated temperatures on mechanical properties of lightweight geopolymer concrete. Case Studies in Construction Materials 15:e00673. https://doi.org/10.1016/j.cscm.2021.e00673
- [71] Aslani F, Asif Z (2019) Properties of ambient-cured normal and heavyweight geopolymer concrete exposed to high temperatures. Materials 12(5):740. https://doi.org/10.3390/ma12050740
- [72] Türkmen İ, Karakoç MB, Kantarcı F, Maraş MM, Demirboğa R (2016) Fire resistance of geopolymer concrete produced from Elazığ ferrochrome slag. Fire Materials 40(6):836-847. https://doi.org/10.1002/fam.2348
- [73] Shaikh F, Vimonsatit V (2015) Compressive strength of fly-ash-based geopolymer concrete at elevated temperatures. Fire Materials 39(2):174-188. https://doi.org/10.1002/fam.2240
- [74] Yang H, Li H, Li C, Yang Q, Jiang J (2024) Biaxial compressive failure criteria and constitutive model of high strength geopolymer concrete after high temperature. Construction Building Materials 426:136165. https://doi.org/10.1016/j.conbuildmat.2024.136165

[75] Zheng Y, Zhang W, Zheng L, Zheng J (2024) Mechanical properties of steel fiber-reinforced geopolymer concrete after high temperature exposure. Construction Building Materials 439:137394. https://doi.org/10.1016/j.conbuildmat.2024.137394

[76] Verma M, Meena RK, Singh I, Gupta N, Saxena KK, Reddy MM, Salem KH, Salmaan U (2023) Investigation on the impact of elevated temperature on sustainable geopolymer composite. Advances in Mechanical Engineering 15(9):16878132231196402. https://doi.org/10.1177/16878132231196402